LETTERS

Redox evolution of a degassing magma rising to the surface

Alain Burgisser[1] & Bruno Scaillet[1]

Volatiles carried by magmas, either dissolved or exsolved, have a fundamental effect on a variety of geological phenomena, such as magma dynamics[1–5] and the composition of the Earth's atmosphere[6]. In particular, the redox state of volcanic gases emanating at the Earth's surface is widely believed to mirror that of the magma source, and is thought to have exerted a first-order control on the secular evolution of atmospheric oxygen[6,7]. Oxygen fugacity (f_{O_2}) estimated from lava or related gas chemistry, however, may vary by as much as one log unit[8–10], and the reason for such differences remains obscure. Here we use a coupled chemical–physical model of conduit flow to show that the redox state evolution of an ascending magma, and thus of its coexisting gas phase, is strongly dependent on both the composition and the amount of gas in the reservoir. Magmas with no sulphur show a systematic f_{O_2} increase during ascent, by as much as 2 log units. Magmas with sulphur show also a change of redox state during ascent, but the direction of change depends on the initial f_{O_2} in the reservoir. Our calculations closely reproduce the H_2S/SO_2 ratios of volcanic gases observed at convergent settings, yet the difference between f_{O_2} in the reservoir and that at the exit of the volcanic conduit may be as much as 1.5 log units. Thus, the redox state of erupted magmas is not necessarily a good proxy of the redox state of the gases they emit. Our findings may require re-evaluation of models aimed at quantifying the role of magmatic volatiles in geological processes.

Recent studies have investigated the role of redox equilibria during volatile exsolution, but the solution of the numerical problem requires fixing either iron or sulphur redox states[11]: as a result, the effect of decompression on f_{O_2} cannot be evaluated. In the present work, we relax such an assumption by taking advantage of the fact that the solubility laws of key volatile species other than H_2O and CO_2 have been recently determined, in particular those of H_2, SO_2 and H_2S (refs 12, 13). We consider gas phases in the system H–O–S, with six species (H_2O, H_2, SO_2, H_2S, S_2 and O_2), in which the following redox equilibria occur:

$$H_2 + \tfrac{1}{2}O_2 = H_2O \quad (1)$$

$$H_2S + \tfrac{1}{2}O_2 = H_2O + \tfrac{1}{2}S_2 \quad (2)$$

$$O_2 + \tfrac{1}{2}S_2 = SO_2 \quad (3)$$

Standard thermodynamic considerations[14,15] show that once total pressure (P), temperature (T), and two additional intensive parameters such as water and hydrogen fugacities (f_{H_2O} and f_{H_2}) are known, the fugacities of all remaining species (f_{H_2S}, f_{O_2}, f_{S_2}, f_{SO_2}) are fixed and the gas phase composition in the H–O–S system is fully determined. Each species i in the gas has a mole fraction m_i: $\sum m_i = 1$.

The gas phase is modelled as an ideal mixture of non-ideal gases, a valid approximation in the pressure range considered here. Departure from ideal behaviour of end-member species is accounted for by the fugacity coefficient γ_i, which is fixed by P and T (ref. 16). The total weight fraction of each species (w_{Ti}) is the sum of its exsolved part (w_{gi}) and its dissolved part: $w_{Ti} = w_{gi} + a_i(\gamma_i m_i P)^{b_i}$, where a_i and b_i are experimentally determined solubility constants (Table 1). We use a homogeneous, one-dimensional conduit flow model[5] to simulate magma ascent under closed-system and equilibrium conditions. Magma rises in a cylindrical conduit at constant mass flux, and volatile exsolution affects the flow through changes in buoyancy and viscosity (see Supplementary Information). Calculations are performed by first fixing P, T, f_{H_2O}, f_{H_2} and the amount of gas in the reservoir. The model seeks first the equilibrium distribution of each volatile species between gas and melt before ascent. Then, at each next lower pressure, mass conservation requires that total amounts of each element (O, H and S) remain constant. Using this constraint, the model calculates the equilibrium distribution of volatile species, which in turn affects ascent dynamics.

Redox equilibrium during magma ascent involving dissolved iron can be written as:

$$Fe_2O_3 = 2FeO + \tfrac{1}{2}O_2 \quad (4)$$

The importance of such a reaction will be dictated by the initial amount of dissolved iron oxides. We have simulated the redox effect of iron by using an empirical model that relates the FeO/Fe_2O_3 ratio of silicate melts to f_{O_2} (ref. 17); here f_{O_2} is referenced to the solid buffer Ni−NiO, such that NNO + 1 means an f_{O_2} one order of magnitude higher than NNO). Runs under typical storage conditions of arc rhyolites (≤1 wt% total iron and f_{O_2} between NNO − 1 and NNO + 1;) show that reaction (4) partly buffers changes in f_{O_2} when little gas is present in the reservoir (<0.2 log units without changing the redox trend during ascent, see Supplementary Information). In contrast, in iron-rich liquids such as basalts, the buffering capacity of iron species will be higher. Thus our results primarily apply to magmas in which the residual melt is rhyolitic, as commonly observed in arc settings. We did not consider the role of iron in crystals because

Table 1 | Solubility constants

Species	a_i	b_i
H_2O	1.063×10^{-3}	0.5399
H_2	3.400×10^{-7}	1.2800
SO_2	1.632×10^{-10}	1.3789
H_2S	8.239×10^{-6}	0.5145
O_2	0	0
S_2	0	0

The parameters a_i and b_i were determined by fitting experimental solubility data of corresponding species to an empirical equation of the form $w_i = a_i f_i^{b_i}$. We have used data from ref. 12 for sulphur-bearing species, from ref. 13 for hydrogen, and from ref. 29 for water.

[1]ISTO, UMR 6113 Université d'Orléans-CNRS, 1a rue de la Férollerie, 45071 Orléans cedex 2, France.

the role of solid buffers as a first-order mechanism controlling redox state during magma ascent can be ruled out on kinetic grounds. The lattice diffusion processes that this mechanism requires are exceedingly slow compared to those in gas or liquid phases.

Similarly, for simplicity we have not investigated the role of CO_2, as detailed petrologic studies of silicic magmas in arcs show them to have little or no CO_2 under pre-eruptive conditions[18]. In general, however, introduction of CO_2 will lower f_{H_2O} and thus drive our calculated values towards lower f_{O_2} via equilibrium (1). Our assumption of equilibrium implies that the model might not capture the chemical evolution of the gas within rapidly decompressed magmas, such as in plinian eruptions, in which the contrasted diffusive kinetics of volatile species may inhibit attainment of equilibrium. Both H_2O and H_2 are, however, fast diffusing species relative to CO_2 and S-bearing ones[18,19]. Thus, if physical fractionation of volatile species arises during ascent, the gas phase composition will be driven towards the system H–O (C and S species remain in the melt, as documented for S for the 1991 Pinatubo eruption[20]), which will exert a dominant control on the redox state of escaping gases. Our model thus represents a fundamental end-member case towards which magmas, notably those andesitic to silicic in arc settings, tend to evolve.

We have explored the following range of starting conditions, typical of silicic arc magmas[21,22]: an initial pressure from 2,000 to 3,000 bar, f_{O_2} from NNO + 2 to NNO − 0.5, bulk iron contents ($FeO^* = FeO + Fe_2O_3/1.113$) up to 3 wt%, bulk water contents up to 10.4 wt% and bulk sulphur contents up to 3 wt%, the last two parameters being adjusted by varying the amount of excess gas in the reservoir (up to 5 wt%; ref. 23). The conduit radius was fixed at 5 m for all runs. Temperature has been fixed to 825 °C, that is, typical of rhyolite magmas[21], and melt density to 2,140 kg m^{-3}, though different choices will not affect the trends observed. Runs are constrained to reach atmospheric pressure at the vent, which yields initial ascent rates between 0.7 and 12 m s^{-1}. Because degassing occurs in equilibrium, changes in chemistry as a function of pressure occur regardless of ascent speed. In all cases, the simulations are carried down to atmospheric pressure, though it can be anticipated that the last increments of f_{O_2} change we compute might not be reached, owing either to the inhibiting effect of viscosity at low water content[24] or to gas loss once a permeability threshold is reached such that the system becomes open to gas[25].

We first consider the S- and Fe-free case. All simulations performed showed essentially identical behaviour in terms of redox state evolution, that is, the f_{O_2} of the magma increases during ascent, the magnitude of increase being more or less damped by the amount of free gas present in the reservoir. A representative example is shown in Fig. 1, corresponding to a magma initially stored at 2,000 bar, at an f_{O_2} of NNO − 0.2, with a melt H_2O content of 5.46 wt%, and for excess gas contents of 0.1, 1 and 5 wt%. The simulations show that the magnitude of f_{O_2} change increases when the amount of excess gas decreases, and can reach more than 2 log units for a gas-poor magma (0.1 wt%).

We now explore the case of S-bearing rhyolite magma with 1 wt% of total iron and stored at 2,000 bar, illustrating our calculations with three different initial f_{O_2} but similar initial dissolved S contents (~200–250 p.p.m.). A magma starting at an f_{O_2} of NNO − 0.5 displays a continuous increase in its f_{O_2} as it ascends, except in the last few hundred bars where a reversal in f_{O_2} towards reduction occurs (Fig. 2). The magnitude of change is strongly dependent on the amount of gas initially present in the reservoir. At low gas content (0.1 wt%), the f_{O_2} rises by 0.7 log units relative to starting conditions. With 5 wt% gas, the magma has a redox state nearly constant up to a pressure of 100 bar. When the starting f_{O_2} in the reservoir is at NNO (Fig. 2), the magma undergoes oxidation only for gas-poor conditions (0.1 wt%). Higher amounts of gas in the reservoir impart a reducing trend in the f_{O_2} evolution during ascent, the final f_{O_2} differing by almost 1 log unit from the initial value for an initial gas content of 5 wt%. When the initial f_{O_2} in the reservoir is at NNO + 1.5, the magma undergoes a significant reduction during ascent regardless of its initial gas content (Fig. 2). In this case, the drop in f_{O_2} may exceed 1.5 log units at near-atmospheric conditions for gas-rich conditions.

The change in f_{O_2} during decompression is accompanied by dramatic changes in gas phase composition (Fig. 3). Our calculated H_2S/SO_2 ratios fall in the range 0.1–10, which is comparable to that of volcanic gases measured at convergent settings for silicic to intermediate magmas[26] (Fig. 3). Clearly, a variety of H_2S/SO_2 ratios can be

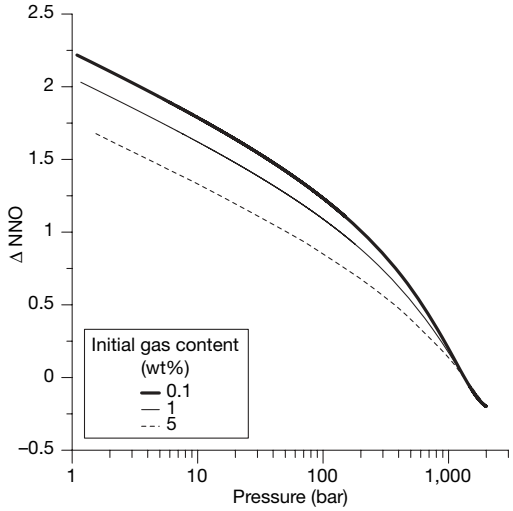

Figure 1 | Fundamental relationship between magma ascent and magma redox state, for a rhyolite magma coexisting with a H–O gas. From gas content and composition at depth, the coupled model of conduit flow calculates the evolution of the physical and chemical conditions of the ascending magma. The effect of equilibrium degassing is a systematic increase in f_{O_2} with decreasing pressure (that is, with shallower depth). Here f_{O_2} is referenced to the solid buffer Ni−NiO (NNO); NNO + 1 means an f_{O_2} one order of magnitude higher than NNO, and is expressed as ΔNNO = 1). The figure shows representative cases, for three initial values of exsolved volatiles with an f_{H_2} initially fixed at 10 bar.

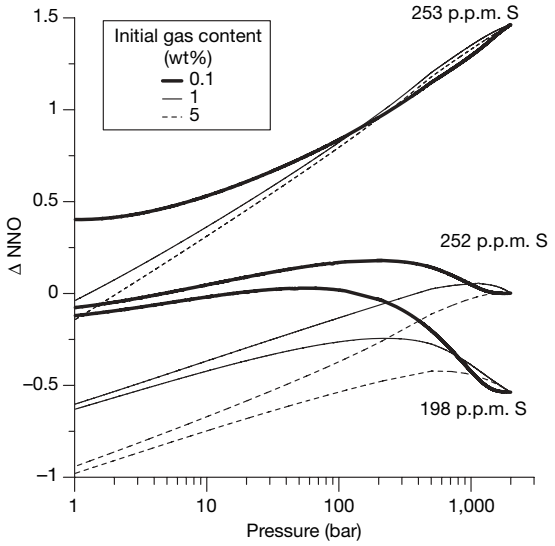

Figure 2 | Fundamental relationship between magma ascent and magma redox state, for a rhyolite magma coexisting with a H–O–S gas. The effect of initial redox state on its evolution during decompression is shown. The graph shows representative cases, for three initial values of exsolved volatiles with an f_{H_2O} initially fixed at 1,000 bar. The initial redox state was achieved by varying f_{H_2} (ΔNNO = −0.5, f_{H_2} = 10; ΔNNO = 0, f_{H_2} = 5.38; ΔNNO = +1.5, f_{H_2} = 1).

produced from magmas having common initial redox states but different amounts of gases. Conversely, a given H_2S/SO_2 ratio may be produced from a wide range of starting redox conditions. For instance, a H_2S/SO_2 ratio of about one can be produced from a magma initially stored at NNO + 1.5 with 5 wt% gas, or from a magma initially at NNO − 0.5 with 0.1 wt% gas (Fig. 3a). Thus, anticipating the H_2S/SO_2 ratio of gases emanating from a given reservoir would require knowing not only the reservoir f_{O_2}, but also the amount of free gas present in the reservoir and the depth at which gas and melt are physically separated. Although such a rich behaviour precludes a simple explanation for each trend calculated, a sensitivity analysis of our model suggests that water exsolution plays an important role in oxidizing the system, and that, on the other hand, the complex pressure dependence of the redox equilibria (1)–(3) contribute to the reducing trends. Our findings have thus obvious implications for the use of volcanic gases as a monitoring tool of volcanic activity. They also illustrate the important role of sulphur. Magmas poor in sulphur or in which reactions involving sulphur are kinetically inhibited are likely to undergo a significant increase in their redox state during ascent.

The above results show that the redox state that magma records at depth does not necessarily mirror that of its escaping gases, in particular when they are released from levels shallower than the main reservoir. Thus, from a broader perspective, our findings have implications for our understanding of how past volcanic activity may have affected Earth's atmosphere. Current models of the evolution of atmospheric oxygen implicitly assume that the redox state of magmatic rocks can be taken as equal to that of their outgassed products[6,7]. Our calculations show that, for silicic magmas, this assumption holds true only under a restricted set of conditions (for instance, a magma starting at NNO − 0.5 with 1 wt% gas, Fig. 2). Oxidized silicic magmas are particularly prone to redox change during ascent. A recent study[10] has stressed the difference in f_{O_2} retrieved from volcanic gas[11] and volcanic glass[12] at Kilauea volcano: the basaltic glass, which is fully degassed, records an f_{O_2} that is 1.2 log units lower than that of the gas. Although our model is calibrated on Fe-poor liquids, its predictions are qualitatively in accord with such an observation, which suggests that even for basaltic magmas in non-arc settings, redox change during degassing may occur[27]. The corollary is that the iron redox state of a magma may differ significantly from that of its source, in contrast to conventional wisdom[28]. Altogether, this suggests that equating the redox state and composition of present-day volcanic gases to those emitted in the geologic past[6] may not be a correct assumption.

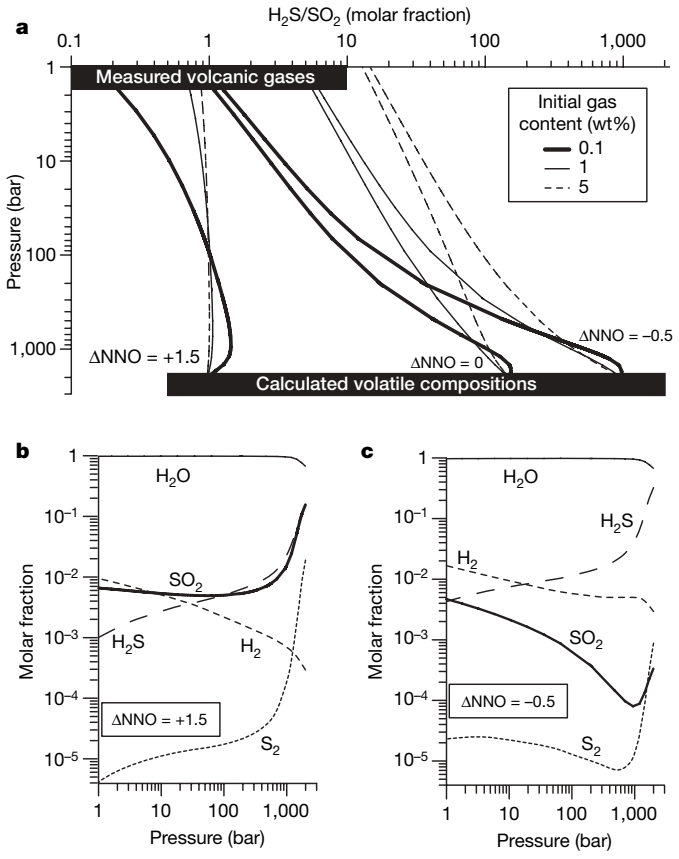

Figure 3 | Evolution of the composition of an H–O–S gas during ascent of a rhyolite magma. a, Effect of the initial redox state on the ratio H_2S/SO_2 for three starting values of f_{O_2}, each with three different gas contents (same initial conditions as in Fig. 2). Also shown are the natural range observed on active volcanoes in convergent settings[26], and the range calculated by phase equilibria experiments[21]. **b**, Evolution of the gas composition for a magma oxidized at depth (ΔNNO = +1.5, 0.1 wt% gas). **c**, Evolution of the gas composition for a magma reduced at depth (ΔNNO = −0.5, 0.1 wt% gas). Contents of O_2 are too low (<10 p.p.m.) to be displayed.

Received 3 April; accepted 28 November 2006.

1. Wilson, L., Sparks, R. S. J. & Walker, G. P. L. Explosive volcanic eruptions. IV. The control of magma properties and conduit geometry on eruption column behavior. *Geophys. J. R. Astron. Soc.* **63,** 117–148 (1980).
2. Papale, P. Strain-induced magma fragmentation in explosive eruptions. *Nature* **397,** 425–428 (1999).
3. Huppert, H. E. & Woods, A. W. The role of volatiles in magma chamber dynamics. *Nature* **420,** 493–495 (2002).
4. Gonnerman, H. M. & Manga, M. Explosive volcanism may not be an inevitable consequence of magma fragmentation. *Nature* **426,** 432–435 (2003).
5. Burgisser, A. & Gardner, J. Experimental constraints on degassing and permeability in volcanic conduit flow. *Bull. Volc.* **67,** 42–56 (2005).
6. Holland, H. D. Volcanic gases, black smokers and the great oxidation event. *Geochim. Cosmochim. Acta* **66,** 3811–3826 (2002).
7. Kasting, J. F., Eggler, D. H. & Raeburn, S. P. Mantle redox evolution and the oxidation state of the atmosphere. *J. Geol.* **101,** 245–257 (1993).
8. Gerlach, T. M. Comment on paper 'Morphology and compositions of spinel in Pu'u'O'o lava (1996–1998), Kilauea volcano, Hawaii'–enigmatic discrepancies between lava and gas-based fO_2 determinations of Pu'u'O'o lava. *J. Volcanol. Geotherm. Res* **134,** 241–244 (2004).
9. Gerlach, T. M. Oxygen buffering of Kilauea volcanic gases and the oxygen fugacity of Kilauea basalt. *Geochim. Cosmochim. Acta* **57,** 795–814 (1993).
10. Roeder, P. L., Thornber, C., Proustovetov, A. & Grant, A. Morphology and composition of spinel in Pu'u'O'o lava (1996–1998), Kilauea volcano, Hawaii. *J. Volcanol. Geotherm. Res.* **123,** 245–265 (2003).
11. Moretti, R. & Papale, P. On the oxidation state and volatile behavior in multicomponent gas-melt equilibria. *Chem. Geol.* **213,** 265–280 (2004).
12. Clemente, B., Scaillet, B. & Pichavant, M. The solubility of sulphur in hydrous rhyolitic melts. *J. Petrol.* **45,** 2171–2196 (2004).
13. Gaillard, F., Schmidt, B., Mackwell, S. & McCammon, C. Rate of hydrogen–iron redox exchange in silicate melts and glasses. *Geochim. Cosmochim. Acta* **67,** 2427–2441 (2003).
14. Holloway, J. R. Thermodynamic modelling of geological materials: minerals, fluids and melts. *Rev. Mineral.* **17,** 211–233 (1987).
15. Scaillet, B. & Pichavant, M. Role of fO_2 on fluid saturation in oceanic basalt. *Nature* **430,** doi:10.1038/nature02814 (published online 28 July 2004).
16. Shi, P. F. & Saxena, F. K. Thermodynamic modeling of the C-H-O-S fluid system. *Am. Mineral.* **77,** 1038–1049 (1992).
17. Kress, V. C. & Carmichael, I. S. E. The compressibility of silicate liquids containing Fe_2O_3 and the effect of composition, temperature, oxygen fugacity and pressure on their redox states. *Contrib. Mineral. Petrol.* **108,** 82–92 (1991).
18. Wallace, P. Volatiles in subduction zone magmas: concentrations and fluxes based on melt inclusion and volcanic gas data. *J. Volcanol. Geotherm. Res.* **140,** 217–240 (2004).
19. Watson, E. B. Diffusion in volatile-bearing magmas. *Rev. Mineral.* **30,** 371–412 (1994).
20. Westrich, H. R. & Gerlach, T. M. Magmatic gas source for the stratospheric SO_2 cloud from the June 15, 1991 eruption of Mount Pinatubo. *Geology* **20,** 867–870 (1992).
21. Scaillet, B. & Pichavant, M. Experimental constraints on volatile abundances in arc magmas and their implications for degassing processes. *Spec. Publ. Geol. Soc. (Lond.)* **213,** 23–52 (2003).
22. Scaillet, B., Luhr, J. & Carroll, M. R. in *Volcanism and the Earth's Atmosphere* (eds Robock, A. & Oppenheimer, C.) 11–40 (Geophys. Monogr. 139, American Geophysical Union, Washington DC, 2003).
23. Wallace, P., Anderson, A. T. & Davis, A. M. Quantification of pre-eruptive exsolved gas contents in silicic magmas. *Nature* **377,** 612–616 (1995).

24. Gardner, J. E., Hilton, M. & Carroll, M. R. Bubble growth in highly viscous silicate melts during continuous decompression from high pressure. *Geochim. Cosmochim. Acta* **64,** 1473–1483 (2000).
25. Eichelberger, J. C., Carrigan, C. R., Westrich, H. R. & Price, R. H. Non explosive silicic volcanism. *Nature* **323,** 598–602 (1986).
26. Symonds, R. B., Rose, W. I., Bluth, G. J. S. & Gerlach, T. M. Volcanic-gas studies: methods, results, and applications. *Rev. Mineral.* **30,** 1–66 (1994).
27. Mathez, E. A. Influence of degassing on oxidation states of basaltic magmas. *Nature* **310,** 371–375 (1984).
28. Carmichael, I. S. E. The redox states of basic and silicic magmas: a reflexion of their source regions. *Contrib. Mineral. Petrol.* **106,** 129–141 (1991).
29. Holtz, F., Behrens, H., Dingwell, D. B. & Johannes, W. H_2O solubility in haplogranitic melts: compositional, pressure and temperature dependence. *Am. Mineral.* **80,** 94–108 (1995).

Supplementary Information is linked to the online version of the paper at www.nature.com/nature.

Acknowledgements We thank M. Rutherford and P. Wallace for comments that helped us to improve our model. A.B. acknowledges support from the Swiss National Science Foundation.

Author Contributions A.B. incorporated the thermodynamic code of gas–melt equilibria developed by B.S. into his one-dimensional conduit flow model. A.B. performed all the simulations. Both authors contributed equally to the interpretation of the model results and to the writing of the paper.

Author Information Reprints and permissions information is available at www.nature.com/reprints. The authors declare no competing financial interests. Correspondence and requests for materials should be addressed to A.B. (burgisse@cnrs-orleans.fr).